Biosensors and Bioelectronics 42 (2013) 409–414

Contents lists available at SciVerse ScienceDirect

Biosensors and Bioelectronics

journal homepage: www.elsevier.com/locate/bios

A chronocoulometric LNA sensor for amplified detection of K-ras mutation based on site-specific DNA cleavage of restriction endonuclease

Liqing Lin [a], Ailin Liu [a], Chengfei Zhao [a], Shaohuang Weng [a], Yun Lei [a], Qicai Liu [a,b], Xinhua Lin [a,*], Yuanzhong Chen [a,c,**]

[a] Department of Pharmaceutical Analysis, Faculty of Pharmacy, Fujian Medical University, Fuzhou 350004, China
[b] Department of Laboratory Medicine, First Affiliated Hospital of Fujian Medical University, Fuzhou 350005, China
[c] Fujian Key Lab of Hematology, Fujian Institute of Hematology, the Affiliated Union Hospital of Fujian Medical University, Fuzhou 350000, China

ARTICLE INFO

Article history:
Received 7 August 2012
Received in revised form
26 September 2012
Accepted 27 September 2012
Available online 26 October 2012

Keywords:
Chronocoulometric LNA sensor
Site-specific DNA cleavage
K-ras mutation
RuHex

ABSTRACT

An amplified chronocoulometric Locked nucleic acid (LNA) sensor (CLS) for selective electrochemical detection of K-ras mutation was developed based on site-specific DNA cleavage of restriction endonuclease EcoRI. Thiolated-hairpin LNA probe with palindrome structure of stem was immobilized on the gold nanoparticles modified gold electrode (NG/AuE). It can be cleaved by EcoRI in the absence of K-ras mutation-type DNA (complementary with the loop part of hairpin probe), but cannot be cleaved in the presence of mutation-type DNA. The difference before and after enzymatic cleavage was then monitored by chronocoulometric biosensor. Electrochemical signals are generated by chronocoulometric interrogation of Hexaammineruthenium (III) chloride (RuHex) that quantitatively binds to surface-confined hairpin LNA probe via electrostatic interactions. The results suggested this CLS had a good specificity to distinguish the K-ras mutation-type, wild-type and non-complementary sequence. There was a good linear relationship between the charge and the logarithmic function of K-ras mutation-type DNA concentration. The detection limit had been estimated as 0.5 fM. It is possible to qualitatively and quantitatively detect K-ras point mutation in pancreatic cancer.

1. Introduction

Carcinoma of the pancreas (PC) is an aggressive disease and the fourth most common cause of cancer death across the globe (Hariharan et al., 2008). PC is sometimes referred to as a "silent killer" because early PC often does not cause symptoms, and the later symptoms are usually nonspecific and varied. Therefore, PC is often not diagnosed until it is advanced. Conventional tumor markers, such as CA 19-9, have a high diagnostic sensitivity, but lack specificity and are therefore not suited for detecting early tumors (Berndt et al., 1998; Däbritz et al., 2005). More effective screening techniques are urgently needed to improve the poor prognosis of the disease. PC is among the best-described genetic diseases (Hilgers and Kern, 1999). The K-ras oncogene is one of the three members of the human ras gene family and naturally occurring mutations in the K-ras gene have been localized to codon 12 and 13. This mutation is commonly restricted to codon 12, so is regarded as a 'signature' of PC and probably associated with familial pancreatic adenocarcinoma (Ebert et al., 2001). Gene alterations of the K-ras type can be used as molecular markers to screen for the presence of neoplastic cells in different clinical specimens. Thus, detection of K-ras mutation will afford an early diagnosis and monitor of the disease. Therefore, it is very significant to develop a new effective method for detection of sequence-specific K-ras in PC.

Within recent years, there has been significant progress in developing biosensors for the rapid, cheap and accurate detections of specific gene sequence (Gao et al., 2011). Various sensing strategies have been developed for a specific DNA sequence detection, aiming at the improvement of sensitivity and selectivity of electrochemical detection (Lin et al., 2011). The introduction of nanomaterial could efficiently increase the electrode surface area and enlarge the DNA immobilization amount (Liu et al., 2005). Thus, the construction of nanostructure modified electrode by a simple strategy to achieve the DNA detection with a high sensitivity is highly desirable. Electrodeposition method is one of the mostly used approaches with the advantages of convenience and the wide applications in electrocatalysis and electroanalysis. The development of gold nanostructures by simple electrodeposition method is very attractive for the applications in biosensor.

* Corresponding author at: Department of Pharmaceutical Analysis, Faculty of Pharmacy, Fujian Medical University, Fuzhou 350004, China. Tel./fax: +86 591 22862016.
** Corresponding author at: Fujian Key Lab of Hematology, Fujian Institute of Hematology, Fujian Medical University Union Hospital, Fuzhou 350001, China. Tel.: +86 591 83351966; fax: +86 591 83324116.
E-mail addresses: xhl1963@sina.com (X.H. Lin), chenyz@pub3.fz.fj.cn (Y.Z. Chen).

0956-5663/$ - see front matter © 2012 Elsevier B.V. All rights reserved.
http://dx.doi.org/10.1016/j.bios.2012.09.063

However, due to the complex background such as plasma samples or polymerase chain reaction (PCR) amplicons, practical application of these strategies might be hampered due to substantial background current or relatively poor specificity for the detection of single nucleotide polymorphisms. In order to circumvent this problem, hairpin LNA probe with palindrome structure of stem was introduced for design of a novel chronocoulometric biosensor by combining with site-specific DNA cleavage of restriction endonuclease. In this study we focus on two points about the design of the probe. First, the effect of using LNA. The specificity of LNA has been reported and has attracted wide attention. LNA nucleotides contain a methylene bridge between the 2′-oxygen and the 4′-carbon of the ribose moiety. The covalent bridge results in a very high affinity for DNA and RNA complementary sequences, with each LNA substitution increasing the melting temperatures (T_m) by as much as 3.0 °C to 9.6 °C (James Yang et al., 2007); LNA/DNA hybrids are more destabilized by single-base mismatches than the corresponding DNA/DNA hybrids (Koshkin et al., 1998; Lin et al., 2011). Secondly, the effect of the using site-specific DNA cleavage of restriction endonuclease EcoRI is studied. Restriction endonuclease recognize a specific palindromic sequence of nucleotides (double-stranded DNA) and produce a cut in the DNA (Choudhury et al., 2011; Endo et al., 2010; Van Cleve and Gumport, 1992). The EcoRI cuts palindromic sequence with the sequence 5′-GAATTC-3′. The complementary strand reads the same in the 5′-to-3′ direction. EcoRI makes one cut between the G and A in each of the DNA strands. After the cuts are made, the DNA is held together only by the hydrogen bonds between the four bases in the middle. Hydrogen bonds are weak, and the DNA comes apart. So, the stem of hairpin LNA probe is designed a special palindromic sequence that contains a EcoRI recognition site (5′–GAATTC-3′). Hairpin LNA probe is immobilized on a nanogold electrode. It can be cleaved by EcoRI in the absence of K-ras mutation-type DNA, but cannot be cleaved in the presence of K-ras mutation-type DNA (Scheme 1). The difference before and after enzymatic cleavage is then monitored by the chronocoulometric biosensor. Electrochemical signals are generated by chronocoulometric interrogation of RuHex that quantitatively binds to surface-confined hairpin LNA probe via electrostatic interactions. Previous studies have well demonstrated that binding of RuHex to DNA is completely through electrostatic interaction while free of any duplex intercalation (Zhang et al., 2006; Steel et al., 1998). As a result, redox charge of RuHex is a direct function of the amounts of DNA strands localized at electrode surfaces. Thus we demonstrate that this prototype CLS is simple, stable, reusable, and can sensitively detect femtomolar target DNA with excellent differentiation ability for single nucleotide polymorphisms.

2. Experimental

2.1. Chemicals and apparatus

All oligonucleotides were synthesized by TaKaRa biotechnology Co., Ltd. (Dalian, China), and their base sequences are illustrated in Table 1. Restriction endonuclease EcoRI and EcoRI buffer were obtained from MBI Fermentas (Shanghai, China). $HAuCl_4 \cdot 4H_2O$ was purchased from Sigma (USA). Hexaammineruthenium (III) chloride (RuHex) was purchased from Sigma-Aldrich Corporation (St Louis, MO). Ethylene glycol–terminated thiol ($HS\text{-}(CH_2)_{11}\text{–}EG_2\text{–}OH$, OEG) was purchased from Prochimia (Poland). Tris–(hydroxymethyl) aminomethane was purchased from Cxbio Biotechnology Co. Ltd. (Denmark). Tris (2-carboxyethyl) phosphine hydrochloride (TCEP) was purchased from Sigma-Aldrich (USA). The buffer solutions are as follows: hybridization buffer was the mixture of 100 mM NaCl and 10 mM TE (pH 8.0), buffers for DNA immobilization buffer are the mixture of 10 mM TE, 10 mM TCEP, 100 mM NaCl and 10 mM $MgCl_2$ (pH 7.4). Washing buffer was the mixture of 0.1 M NaCl and 10 mM PB (pH 7.4). Solution contained 0.1 mol/L KCl and 10 mM $Fe(CN)_6^{3-}$/$Fe(CN)_6^{4-}$ was used for electrochemical impedance spectroscopy (EIS) characterization. All solutions were prepared with MilliQ water (18.2 MΩ/cm resistivity) from a Millipore system.

The electrochemical measurements for EIS and chronocoulometry were carried out on a CHI 760d electrochemical working station (CH Instrument Company, USA) using a three-electrode system consisted of a platinum wire as an auxiliary electrode, an Ag/AgCl electrode as reference electrode and a 2 mm diameter Au disk electrode as working electrode. Scanning electron microscope

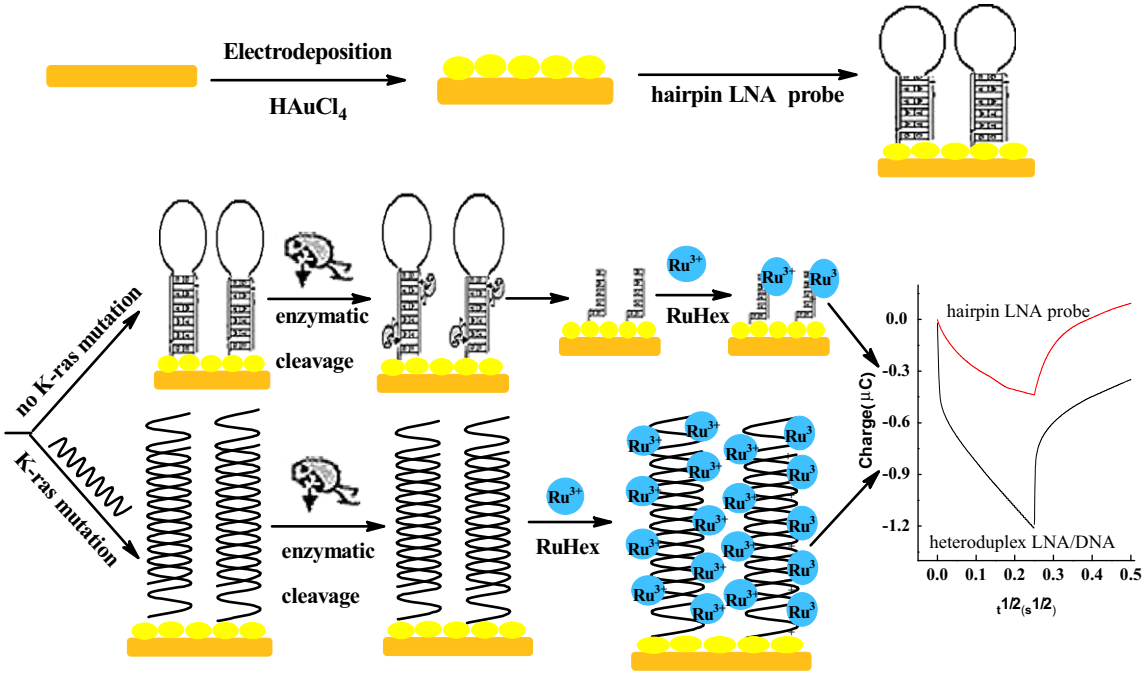

Scheme 1. Schematic representation of the designed strategy for DNA detection.

Table 1
Details of the DNA sequences.

Designation	Sequence (5′–3′)
Thiolated-hairpin LNA probe[a]	SH-aaaagaattcT**A**^{L}C**G**^{L}CC**AACA**^{L}GC**T**^{L}CCAgaattc
wild-type target DNA	TGGAGCT**GGT**GGCGTA
mutation-type target DNA	TGGAGCT**GAT**GGCGTA
non-complementary target DNA	GCTGCAGATTCAATGC

[a] LNA nucleotides contain a methylene bridge between the 2′-oxygen and the 4′-carbon of the ribose moiety. LNA probe is a DNA–LNA chimera, but for brevity it will be called LNA probe. Red bold letters represent LNA bases.

(SEM) (Hitachi S-4800, Japan) was used to examine the morphology of nanogold electrodes.

2.2. Electrode preparation

The whole fabrication process of this biosensor is outlined in Scheme 1. A gold disk electrode (AuE) was firstly polished to obtain mirror surface with 0.05 μm alumina powder, followed by sonication in ethanol and water for 5 min, respectively. Then the gold electrodes were dried with nitrogen gas, and cycled in 0.5 mol/L H_2SO_4 aqueous solution until a stable gold oxide formation/reduction cyclic voltammogram was obtained. The pretreated electrodes were immersed into the $HAuCl_4$ solution containing 0.1 M KNO_3 as electrolyte, where electrochemical deposition was conducted at −200 mV by single potential mode in 6.0 mM $HAuCl_4$ for 5 min to obtain the nanogold modified AuE (NG/AuE).

After drying with nitrogen, the NG/AuE was immediately used for hairpin probe immobilization. Firstly, 5 μL of hairpin LNA probe solution was spread on the NG/AuE surface for 12 h in the 100% humidity. Then, the hairpin LNA probe immobilized electrode was immersed in hybridization buffer containing mutation-type, wild-type or uncomplimentary target DNA, respectively. The hybridization was allowed for 1 h at 47 °C (Lin et al., 2011). After being washed with ice-cold washing buffer, the CLS was incubated with 2 mM OEG for 1 h to repel any possible nonspecific adsorption (Zhang et al., 2008). Afterwards, the sensor was then immersed in EcoRI endonuclease solution (containing EcoRI endonuclease 0.08 units/μL) and rinsed with wash buffer. Add RuHex solution to the electrochemical cell. Purge the solution thoroughly with nitrogen for 10 min through a plastic gas tube. Maintain the solution under nitrogen during subsequent electrochemical measurements by positioning the gas tube above the solution in the electrochemical cell. Placed the modified electrodes in the cell for a certain interval and rinsed with Tris–HCl (pH 7.4), then in 10 mM Tris–HCl solutions for chronocoulometry detection.

2.3. Detection protocol

Electrochemical impedance experiments were performed in the presence of 10 mM $[Fe(CN)_6]^{4-/3-}$. The biased potential was 0.22 V (vs. Ag/AgCl) and the amplitude was 5.0 mV. EIS were recorded in the frequency range of 0.1–10^5 Hz. A Nyquist plot (Zre vs. Zim) was drawn to analyze the impedance results. Perform chronocoulometry measurement with the following parameters: initial potential: 0.2 V; final potential: −0.5 V; number of steps: 2; pulse width: 0.25 s; sensitivity: 1 e^{-3}A/V. Plot charge (Q) versus $t^{1/2}$ and obtain the charge for the hairpin probe modified electrode (Q) from the intercept at $t=0$.

2.4. Detection PCR amplicons of K-ras DNA in real samples

In order to test the real applicability of our new amplified CLS, we challenged it with PCR amplicons for real samples. Templates cDNA of Panc-1 and real samples were kindly donated by First Affiliated Hospital of Fujian Medical University. The PCR amplification was performed in a Bio-Rad PCR cycler. The amplification protocol is as follows, 3 min at 94 °C followed by 20 cycles of 94 °C for 30 s, 58 °C for 30 s, and 72 °C for 30 s. The reaction system was further incubated for 5 min at 72 °C to extend any incomplete products. After PCR amplification and purification, the PCR amplification products from real sample were sent to Shanghai Sangon Biological Engineering Technology Services Reagents Co., Ltd. (China) to determine the sequence. The PCR products were diluted by 10 times with buffer solution and thermally denatured by using a boiling water bath (5 min at +100 °C). The amplicon strands re-annealing was then retarded by cooling the sample in an ice-water bath for 5 min and subjected to electrochemical sensor detection following the same procedure used for synthetic oligonucleotides.

3. Results and discussion

3.1. Characterization of the gold nanoparticles modified gold electrode

In order to immobilize a large amount of hairpin probe on the electrode surface, the gold nanoparticles modified gold electrode was prepared by an electrochemical deposition and then used as the substrate for hairpin probe immobilization and hybridization. Optimize nanogold electrode could be obtained by choosing different solution concentration and different deposition time at −200 mV (Liu et al., 2005). Through optimization, the SEM images of electrodes is shown in Fig. 1: (A) the planar gold electrode; (B) the nanogold electrode obtained by electrodepositing in 6.0 mM $HAuCl_4$ and 0.1 M KNO_3 solution for 5 min at −200 mV. The planar gold electrode surface was comparably smooth and no gold nanoparticles could be seen. The inset Fig. 1 (B) shows that the NG/AuE obtained by electrodepositing consisted of multilayers of gold nanoparticles with a diameter of about 30–55 nm and many voids between particles. This NG/AuE is the optimum electrode for hairpin probe immobilization and hybridization.

The NG/AuE was electrochemically characterized in a solution of 0.5 M H_2SO_4 at a scan rate of 100 mV/s (Fig. 1C, b). For comparison, the cyclic voltammogram of a bare flat gold electrode under the same condition was also presented (Fig. 1C, a). The relative surface area could be evaluated from the coulomb integration of the reductive waves of gold oxide formed in the positive potential scan in 0.5 M H_2SO_4(Gao et al., 2007). It could be deduced that the surface area of NG/AuE is about 4.3 times compared with that of planar gold electrode. This indicated that the current obtained NG/AuE largely increased the effective electrode surface area.

3.2. Electrochemical responses of the biosensor based on NG/AuE

Electrochemical impedance spectroscopy (EIS) can give information on the impedance changes of the electrode surface in the modification process. Fig.2 shows the typical EIS changes for surface-modified process. The semicircle diameter of EIS equals the electron-transfer resistance (R_{et}), which controls the electron-transfer kinetics of the redox-probe at the electrode interface. R_{et} of the bare AuE was estimated to be 102 Ω (Fig. 2a). When the NG was electrodeposited on the surface of the AuE, the NG/AuE exhibited an almost straight line (Fig. 2b). This implies that NG had been successfully modified onto AuE, resulting in the electrode having a larger electroactive surface and higher conductivity. So the presence of NG played an important role in accelerating the transfer of the electrons, thus decreasing the resistance of the

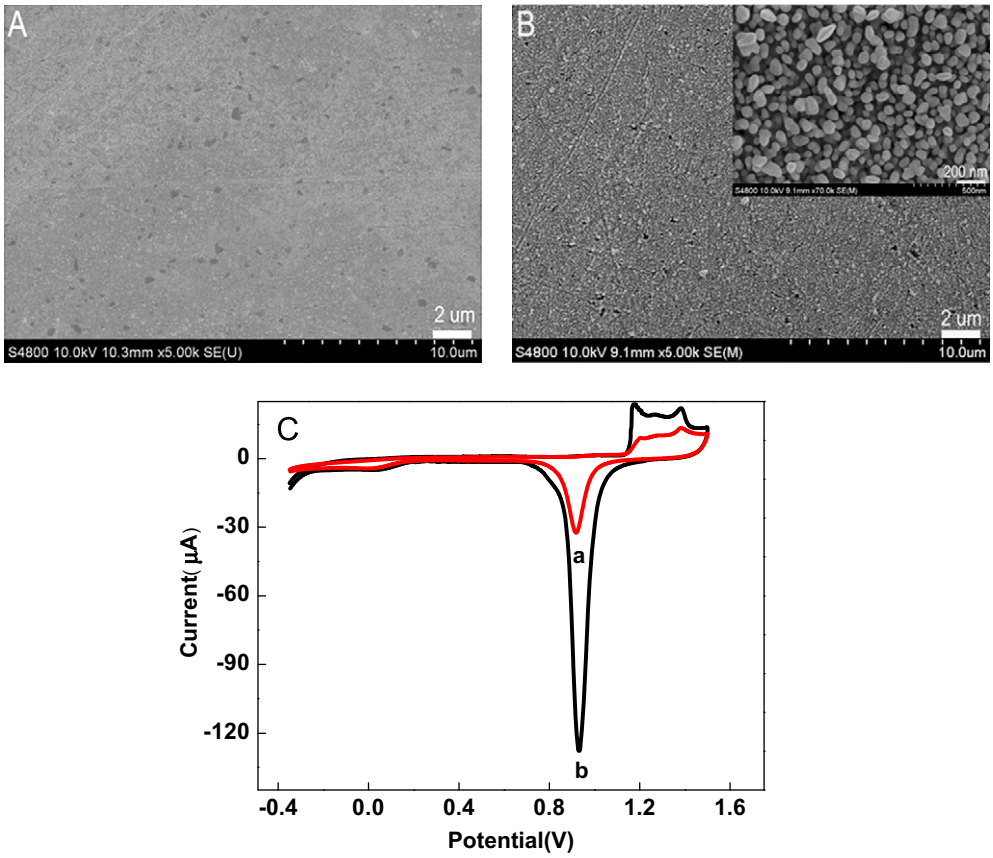

Fig. 1. SEM images of (A) the bare AuE, (B) the NG/AuE obtained by electrodepositing at the potential of −200 mV (vs. Ag/AgCl) in 6 mM $HAuCl_4$ for 5 min, (C) Cyclic voltammogram of the bare AuE (a) and obtained NG/AuE(b) in 0.5 M H_2SO_4 solution.

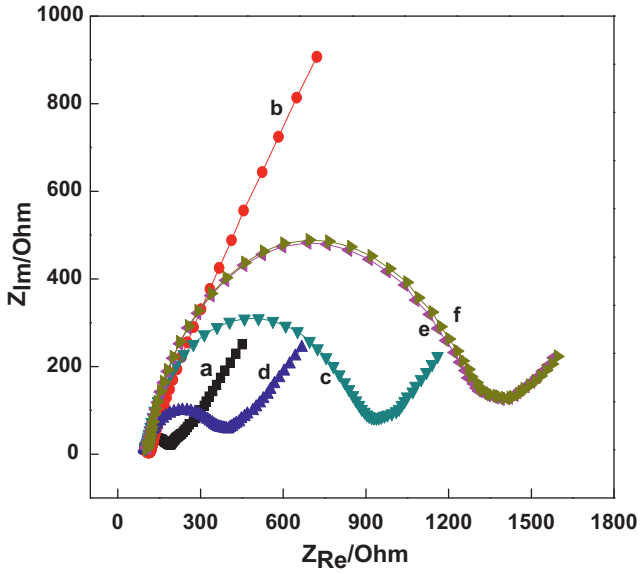

Fig. 2. Impedance spectra (Nyquist plot) of bare AuE (a), NG/AuE (b), hairpin LNA probe/NG/AuE (c), hairpin LNA probe/NG/AuE after being incubated with the EcoRI endonuclease (d), the heteroduplex LNA/DNA modified NG/AuE (e) and heteroduplex LNA/DNA modified NG/AuE after being incubated with the EcoRI endonuclease (f) in the presence of 10 mM $[Fe(CN)_6]^{4-/3-}$. The biased potential was 0.22 V (vs. Ag/AgCl) in the frequency range of 0.1–10^5 Hz.

NG/AuE to $[Fe(CN)6]^{3-/4-}$. After the thiol-functionalised hairpin LNA probes were immobilized on the NG/AuE, its R_{et} value was 917 Ω (Fig. 2c). The large R_{et} value mainly was the negatively charged phosphate backbone of the hairpin probe prevented $[Fe(CN)_6]^{3-/4-}$ from reaching the electrode surface during the redox process, and therefore led to the obvious increase of R_{et} value. After the hairpin probe modified electrode was immersed into the EcoRI endonuclease solution, the R_{et} value was 351 Ω (Fig. 2d). The resistance decrease could be attributed to the fact that the stem duplex of the hairpin probe contains a cleavage site for EcoRI and was subsequently cleaved by this enzyme. The cleavage resulted in the decrease of the negative charges of DNA on the AuE surface. Subsequently, complementary sequence was hybridized with the loop part of hairpin LNA probe (16-base) to form a rigid heteroduplex LNA/DNA modified biosensor, which broke the relatively shorter stem duplex (6-base). At this time, the value of R_{et} increased to 1390 Ω due to large amount of negatively charged DNA linked on the electrode surface (Fig. 2e). When the heteroduplex LNA/DNA modified biosensor was incubated with EcoRI, no significant difference of R_{et} was observed (Fig. 2f). It may be that the formation of rigid duplex DNA of loop sequence essentially does not contain the EcoRI cleave site, which the relatively shorter stem duplex was broken to single strand DNA. Therefore, it cannot be cleaved by EcoRI, which indicated that the hybridization events could be monitored by employing this novel electrochemical strategy.

3.3. The optimize condition and sensitivity of this novel CLS

In order to improve the signal-to-noise ratio and obtain high analytical performance, some important detection parameters were optimized in pure buffer (Fig. S1). Hairpin LNA probe and EcoRI were proposed and employed to improve the specificity. In the presence of EcoRI endonuclease, the chronocoulometric

signals decreased with the increasing incubation time due to more cleavage of the hairpin LNA probes. For sufficient cleavage of the hairpin probes by EcoRI to degrade background signals, 20 min was chosen as the optimal incubation time.

After complementary sequence was hybridized with the loop part of hairpin probe and employing RuHex as the signaling molecule. With the increasing concentration of the RuHex, the chronocoulometric signals increased and tended to a steady value after 40 μM. Considering the sensitivity and dynamic range, 50 μM was chosen as the optimal concentration.

The hairpin LNA probes immobilized on NG/AuE were hybridized with target DNA sequences, then incubated with EcoRI endonuclease for 20 min and rinsed with wash buffer. Prior to chronocoulometry measurement, the modified electrode was immersed in Tris–HCl (pH 7.4) containing 50 μM RuHex for 15 min and rinsed with Tris–HCl, then in 10 mM Tris–HCl solutions for chronocoulometry detection. RuHex serves as the signaling molecule, which binds to anionic phosphate of DNA strands in a stoichiometric approach. We observed that redox charges of RuHex increased upon hybridization with mutation-type (complementary DNA). We then evaluated the detection performance of CLS by exposing the sensor to a series of mutations DNA concentrations. We found that signal intensity was logarithmically related to mutations DNA concentrations (Fig. 3). The linear range for logarithm of mutations DNA was 1 fM-10 pM with the equation of ΔQ (μQ)=0.695+0.185 logC (PM), r=0.9935, The detection limit for DNA detection is estimated to be 0.5 fM. The relative standard deviations (RSD) of the CLS for 10 replicate determination of 1.0×10^{-12} M mutations DNA was 2.8%. This detection limit is lower than the existing electrochemical biosensors based on methylene blue as an electroactive indicator as reporter (Liu et al., 2005).

3.4. Selectivity of this novel CLS

The selectivity of this CLS was investigated by using the hairpin LNA probe to hybridize with the 10 pM concentration of mutation-type DNA, wild-type DNA and the non-complementary DNA sequence in pure buffer, respectively. The hybridized electrodes immersed in Tris–HCl containing 50 μM RuHex for 15 min after treatment with the EcoRI endonuclease, then rinsed with Tris–HCl. The chronocoulometry measurement was carried out in Tris–HCl solutions. The chronocoulometric response of the wild - type (Fig. 4c) had a lower response than that of mutation-type (Fig. 4d). The low response of the hybrid with wild-type comes from a single mismatch, which makes the hybrid unstable. In addition, as expected, nearly no response of chronocoulometric signals can be observed for the hairpin probe (Fig. 4a) hybridization with non-complementary sequence (Fig. 4b), since no successful hybridization occurs due to the sequence mismatch between the hairpin probe and the non-complementary sequence. These results demonstrated that the proposed CLS was able to effectively detect the target with specificity. This high specificity arose from the conformational constraint of the stem–loop structure and site-specific DNA cleavage of EcoRI, that is, the stem of hairpin probe is a special palindrome DNA that contains a EcoRI recognition site.

In order to evaluate the applicability of this CLS in clinically relevant samples, we challenged the sensor performance in human sera. Sera are highly complicated biological fluids containing large amounts of proteins and other molecules. Under these conditions, we could find the CLS still kept high selectivity between 10 pM wild-type and mutation-type sequences in the presence of 10% serum. Significantly, we found that this CLS was highly resistant to serum, with little alteration of the background noise and nearly the same chronocoulometric signal for the 10 pM wild-type sequences even in the presence of 20% serum (Fig. S2). Because OEG-terminated thiols are highly protein-resistant and effectively repel nonspecific adsorption (Prime and Whitesides, 1993). These results suggest the selectivity of the E-DNA sensor is, thus, sufficient to detect and identify target DNA sequences directly in clinically relevant materials.

3.5. Detection of the real PCR sample

In order to test the real applicability of our new CLS, we further challenged it with a PCR amplicon from the real sample. The

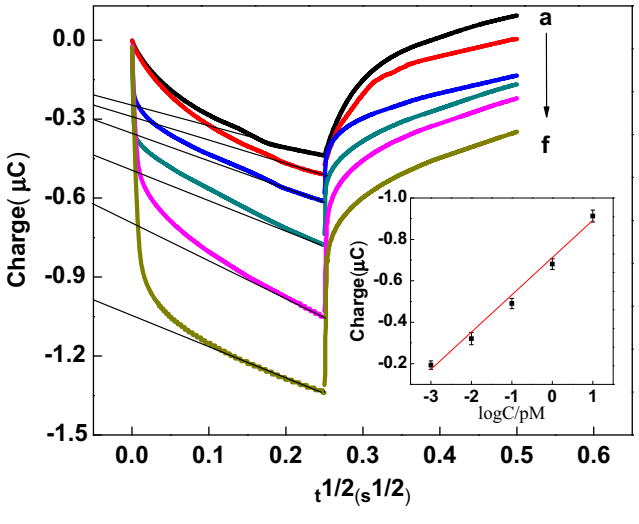

Fig. 3. Chronocoulometric curves for hairpin LNA probe modified NG/AuE before and after hybridization with mutation-type DNA (complementary) at a series of concentrations (from a to f: 0, 1 fM, 10 fM, 100 fM, 1 pM and 10 pM) were obtained in 10 mM Tris buffer (pH 7.4) after treatment with the EcoRI endonuclease. Pulse width: 0.25 s. Intercepts at t=0 in chronocoulometric curves represent redox charges of RuHex bound to DNA. Inset is logarithmic plot of signal vs. complementary DNA concentration.

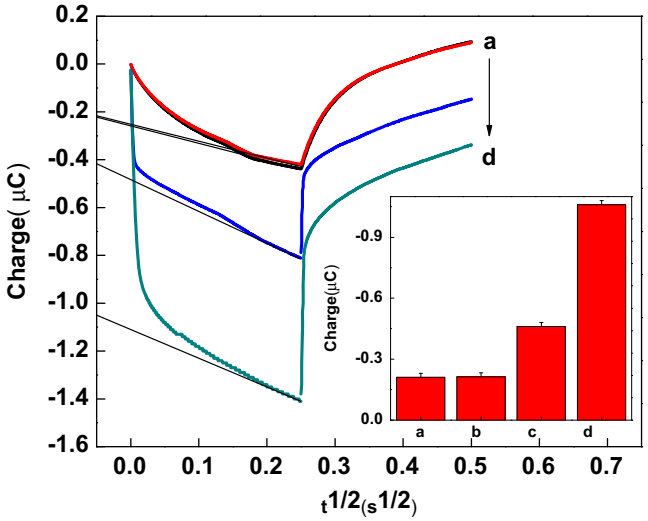

Fig. 4. Chronocoulometric signals of hairpin probe modified NG/AuE (a) and after hybridization with mutation-type (d), wild-type (c) and non-complementary sequence (b) were obtained in 10 mM Tris buffer (pH 7.4) after treatment with the EcoRI endonuclease. Inset shows the bar graph of the chronocoulometric signal when the hairpin probe hybridized with different DNA sequence. Error bars, ± relative standard deviation of three independent experiments.

measured gene sequences result of real sample PCR amplicon were shown in Fig. S3. We obtained the target sequences that could be directly sensed by hairpin probe. The denatured fragment from real sample was applied to the CLS detection after PCR amplification. Fig.S4 shows the chronocoulometric signals when the hairpin probes were immobilized and hybridized with real PCR samples in the hybridization step. The results showed that the CLS was a promising tool for the sensitive and portable detection of PC.

4. Conclusions

In summary, we have introduced here an amplified strategy for development of CLS based on hairpin LNA probe and site-specific DNA cleavage of restriction endonuclease. This CLS based on nanogold electrodeposition was used to detect DNA species related to K-ras of PC. The results illustrated that the proposed CLS has the advantages of higher sensitivity and lower background current. Given the simplicity in design of the proposed CLS, it is fairly easy to generalize this strategy to detect a K-ras mutation. We employed this sensor to directly detect PCR amplicons from real samples with satisfactory results. So this CLS is a promising tool for the sensitive and portable detection K-ras mutation of PC.

Acknowledgment

We gratefully acknowledge the financial support of the National High Technology and Development of China (863 Project: 2012AA022604), the National Natural Science Foundation of China (21275028, 81171668, 81201362 and 20975021), the Fujian Provincial University-Industry Cooperation Sciecne & Technology Major Program (2010Y4003), the Natural Science Foundation of Fujian Province (2009J01023, 2010J06011, 2010J01032), the Scientific Research Major Program of Fujian Medical University (09ZD013) and the Foundation of Fujian Education Department (JA10155, JA12130).

Appendix A. Supporting information

Supplementary data associated with this article can be found in the online version at http://dx.doi.org/10.1016/j.bios.2012.09.063.

References

Berndt, C., Haubold, K., Wenger, F., Brux, B., Muller, J., Bendzko, P., Hillebrand, T., Kottgen, E., Zanow, J., 1998. Clinical Chemistry 44, 2103–2107.
Choudhury, J.R., Rao, L., Bierbach, U., 2011. Journal of Biological Inorganic Chemistry 16, 373–380.
Däbritz, J., Hänfler, J., Preston, R., Stieler, J., Oettle, H., 2005. British Journal of Cancer 92, 405–412.
Ebert, M., Schandl, L., Scmid, R., 2001. Digestive Diseases and Sciences 19, 32–36.
Endo, M., Katsuda, Y., Hidaka, K., Sugiyama, H., 2010. Journal of the American Chemical Society 132, 1592–1597.
Gao, W.C., Dong, H.F., Lei, J.P., Ji, H.X., Ju, H.X., 2011. Chemical Communications 47, 5220–5222.
Gao, W., Xia, X.H., Xu, J.J., Chen, H.Y., 2007. Journal of Physical Chemistry C 111, 12213–12219.
Hariharan, D., Saied, A., Kocher, H.M., 2008. HPB 10, 58–62.
Hilgers, W., Kern, S.E., 1999. Genes, Chromosomes and Cancer 26, 1–12.
James Yang, C.Y., Wang, L., Wu, Y.R., Kin, Y.M., Medley, C.D., Lin, H., Tan, W.H., 2007. Nucleic Acids Research 35, 4030–4041.
Koshkin, A.A., Rajwanshi, V.K., Wengel, J., 1998. Tetrahedron Letters 39, 4381–4384.
Lin, L.Q., Liu, Q.C., Wang, L.M., Liu, A.L., Weng, S.H., Lei, Y., Chen, W., Lin, X.H., Chen, Y.Z., 2011. Biosensors and Bioelectronics 28, 277–283.
Liu, S.F., Li, Y.F., Li, J.R., Jiang, L., 2005. Biosensors and Bioelectronics 21, 789–795.
Prime, K.L., Whitesides, G.M., 1993. Journal of the American Chemical Society 115, 10714–10721.
Steel, A.B., Herne, T.M., Tarlov, M.J., 1998. Analytical Chemistry 70, 4670–4677.
Van Cleve, M.D., Gumport, R.I., 1992. Biochemistry 31, 334–339.
Zhang, J., Song, S.P., Zhang, L.Y., Wang, L.H., Wu, H.P., Pan, D., Fan, C.H., 2006. Journal of the American Chemical Society 128, 8575–8580.
Zhang, J., Lao, R.J., Song, S.P., Yan, Z.Y., Fan, C.H., 2008. Analytical Chemistry 80, 9029–9033.